On the interpretation of Michelson–Morley experiments

Claus Lämmerzahl[1] and Mark P. Haugan[2]
[1] Institute for Experimental Physics, Heinrich–Heine–University Düsseldorf, 40225 Düsseldorf, Germany
[2] Purdue University, West Lafayette, IN 47907, USA

February 5, 2008

Abstract

Recent proposals for improved optical tests of Special Relativity have renewed interest in the interpretation of such tests. In this paper we discuss the interpretation of modern realizations of the Michelson–Morley experiment in the context of a new model of electrodynamics featuring a vector–valued photon mass. This model is gauge invariant, unlike massive–photon theories based on the Proca equation, and it predicts anisotropy of both the speed of light and the electric field of a point charge. The latter leads to an orientation dependence of the length of solid bodies which must be accounted for when interpreting the results of a Michelson–Morley experiment. Using a simple model of ionic solids we show that, in principle, the effect of orientation dependent length can conspire to cancel the effect of an anisotropic speed of light in a Michelson–Morley experiment, thus, complicating the interpretation of the results.

keywords: Michelson–Morley experiment, isotropy of space, Maxwell equations, test of Special Relativity

PACS: 03.30.+p, 03.50 De

1 Introduction

The Michelson–Morley experiment [1] is one of the most famous physics experiments ever performed, and it has a unique place in both the history and the empirical foundations of Special Relativity. Originally conceived as a test for the existence of the ether, a medium that was to carry electromagnetic waves and whose rest frame would realize Newton's absolute space, the experiment's failure to detect the expected anisotropy of the speed of light in a frame moving through the ether presented physicists with the puzzle eventually solved by Einstein's Special Theory of Relativity [2]. Subsequently, Robertson developed a kinematical test theory [3] in which he could show that the null results of the Michelson–Morley and Kennedy–Thorndike experiments in combination with the result of the time–dilation experiment of Ives and Stilwell thoroughly tested the validity of Special Relativity.

The original Michelson–Morley experiment [1] exploited an interferometer in which a light beam was split into two beams propagating back and forth along perpendicular paths of equal length. It was expected that when the interferometer was rotated interference of the recombined beams would show the effects of an anisotropy of the speed of light caused by the Earth's motion through the ether. The experiment's failure to detect this effect had an impact on physicists of the day that is difficult to appreciate fully now.

Modern realizations of the Michelson–Morley experiment generally exploit microwave cavities. For example, Brillet and Hall [4] mounted such a cavity on a rotating table. Any orientation dependence of the speed of light would lead to a corresponding orientation dependence of the frequency of microwaves resonant with the cavity. The null result of the Brillet–Hall experiment, which looked for such dependence, constrains any anisotropy of the speed of light to be less than a part in 10^{15}, that is, $\delta c/c \lesssim 10^{-15}$. Proposed space–based versions of the Michelson–Morley experiment called SUMO

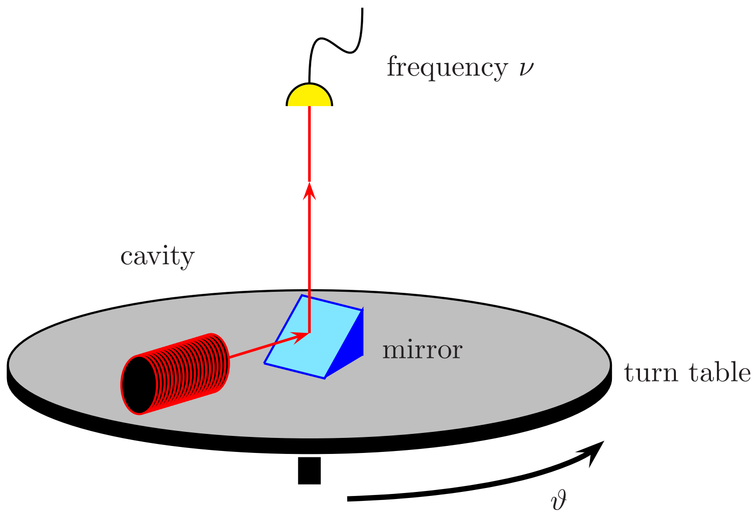

Figure 1: A schematic view of Michelson–Morley experiment using a cavity.

[5] and OPTIS [6], which exploit cryogenic and room–temperature cavity resonators, respectively, are capable of tightening this already impressive constraint by several orders of magnitude. The prospect of such precise new tests motivates our reexamination of their meaning for the empirical foundations of Special Relativity.

Elementary considerations establish that the angular frequencies of electromagnetic waves resonant within a cavity of length L are $\omega = ck$, where $k = \pi n/L$, $n = 1, 2, 3, \ldots$, denotes the wave number of the resonant wave. Clearly, any orientation dependence of the speed of light, $c = c(\vartheta)$, leads to a corresponding orientation dependence of the resonant frequencies,

$$\omega(\vartheta) = c(\vartheta)\frac{n\pi}{L} \,. \tag{1}$$

See Fig. 1 for a simple experimental setup sensitive to this sort of dependence.

From the form of (1) it is clear that an orientation dependence of the length of a cavity would also contribute to an orientation dependence of resonant frequencies. In this Letter we show that consistent, physically motivated dynamical models can predict both an orientation dependence of the length of solid bodies and an anisotropy of the speed of light, thus, complicating the interpretation of the results of Michelson–Morley experiments. For the particular model we analyze below that these competing influences on a cavity's resonant frequencies can conspire to cancel. However, we also show that this cancellation is negligible in Michelson–Morley experiments performed to date or in proposed new versions of the experiment. The familiar interpretation of the results of these experiments remains valid.

In the following we describe the dynamical model that is the basis for our analysis, show that it predicts both an anisotropic speed of light and an orientation dependent length of crystalline structures and demonstrate that only when both of these effects are accounted for does one obtain a reliable interpretation of the results of Michelson-Morley experiments.

2 An alternative model of electrodynamics

Designing and interpreting the results of experimental tests of Special Relativity requires that one consider consistent, physically reasonable alternatives to familiar relativistic dynamics. In proposing an alternative electrodynamics based on modified Maxwell equations we aim to explore the consequences of conceivable departures from special relativistic physics. We make no special claim for the correctness of any particular alternative that we consider. We do show that these alternatives

can lead not only to an anisotropic speed of light but also to an anisotropy in the electromagnetic interactions that affects the structure of solids. Only when both of these effects are accounted for does one obtain a reliable interpretation of the results of Michelson–Morley experiments.

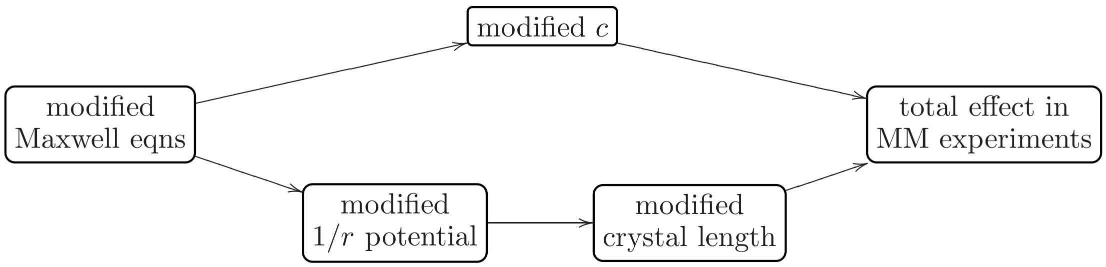

2.1 The modified Maxwell equations

A constructive approach to Maxwell's equations [7, 8, 9, 10] suggests the following general structure for equations of motion governing the dynamics of the electromagnetic field,

$$4\pi j^a = \underbrace{\chi^{abcd}\partial_b F_{cd}}_{\text{structure of null cones}} + \underbrace{\chi^{acd}F_{cd}}_{\text{mass–term}} . \tag{2}$$

Here $F_{ab} = \partial_a A_b - \partial_b A_a$ denotes the tensor of electromagnetic field strengths with A_a the electromagnetic 4–potential. Recent speculations regarding modifications of electrodynamics induced by quantum gravity are consistent with this general structure (2), see [9] for a review.

The first term on the right–hand side of (2) governs the propagation of field discontinuities and thus defines the light–cones. The factor χ^{abc} in the second term acts like a sort of tensorial photon mass. It gives rise to dispersion and to a Yukawa–like form of the field of a point charge (see below). Note that equation (2) is manifestly gauge invariant. In contrast, models of a massive photon based on the Proca equation break gauge invariance [11].

In this Letter we consider the following simple case of the equations (2),

$$4\pi j^b = \partial_a F^{ab} + \theta_a F^{ab} , \tag{3}$$

where $\chi^{abcd} = \eta^{a[c}\eta^{d]b}$ and $\chi^{acd} = \eta^{ad}\theta^c$ with η^{ab} the usual Minkowski metric $\eta^{ab} = \mathrm{diag}(+---)$. The factor θ_a acts like a sort of vectorial photon mass, though it might reflect properties of the vacuum or the value of a background field rather than an intrinsic property of the photon [10]. Because of the empirical successes to date of the familiar Maxwell's equations, we expect the magnitudes of the components θ_a to be small in a laboratory in the Earth's neighborhood.

A 3+1 decomposition of our modified Maxwell equations (3) yields

$$4\pi\rho = \boldsymbol{\nabla}\cdot\boldsymbol{E} + \boldsymbol{\theta}\cdot\boldsymbol{E} \tag{4}$$

$$\frac{4\pi}{c}\boldsymbol{j} = \frac{1}{c}\partial_t\boldsymbol{E} + \boldsymbol{\nabla}\times\boldsymbol{B} - \frac{1}{c}\theta_0\boldsymbol{E} + \boldsymbol{\theta}\times\boldsymbol{B} . \tag{5}$$

where, as usual, $E_i = F_{0i}$ and $B_i = F_{jk}$, for cyclic i, j and k, and where the units of θ_0 and $\boldsymbol{\theta}$ are sec^{-1} and m^{-1}, respectively. The physical significance of the speed–of–light parameter c is discussed below. Note that, in general, charge is not conserved. However, this implies no inconsistency of our model [10] and is, conceivably, a desirable feature in brane worlds where matter can tunnel to the bulk [12].

Experimental constraints on a hypothetical photon mass are quite severe. The tightest constraint from a laboratory experiment is $m \leq 10^{-47}$ g, see [13], while the constraint $m \leq 10^{-48}$ g is inferred from measurements of the earth's magnetic field. Recent astrophysical observations of electromagnetic radiation of vastly different frequencies emitted by GRBs imply the constraint $m \leq 10^{-49}$ g, see [14]. We see below that these constraints on m are equivalent to constraints on $|\boldsymbol{\theta}|\hbar/(2c)$.

We are interested in laboratory experiments conducted within limited regions of spacetime so we will treat θ_a as constant in the following. In the case of timelike θ_a there is a preferred frame in which only the θ_0 component is nonzero and in which electrodynamics is isotropic. In a frame moving with velocity $\boldsymbol{w}$ relative to this preferred frame $\boldsymbol{\theta}$ is roughly $\theta_0 \boldsymbol{w}$. This case falls within the range of possibilities considered kinematically by Robertson [3]. The case of a spacelike θ_a, in which there is a preferred frame in which θ_0 vanishes and electrodynamics is intrinsically anisotropic, does not.

2.2 Plane electromagnetic waves

The wave equation that follows from (3) is

$$4\pi\partial_{[a}j_{b]} = \frac{1}{2}\left(\Box F_{ba} + \theta^c\partial_c F_{ba}\right). \tag{6}$$

For a plane wave, $F_{ab} = F^0_{ab}e^{-ik_c x^c}$, it implies the dispersion relation

$$\eta^{ab}k_a k_b + i\theta^a k_a = 0\,. \tag{7}$$

Solving for the wave's angular frequency we find

$$\omega = -\frac{i}{2}\theta^0 \pm c\sqrt{\boldsymbol{k}^2 - i\theta^{\hat{a}}k_{\hat{a}} - \frac{1}{4}(\theta^0)^2}\,. \tag{8}$$

which, in the physically interesting limit of small θ_a, is approximately

$$\omega \approx \pm c|\boldsymbol{k}|\left(1 + \frac{1}{8|\boldsymbol{k}|^2}((\boldsymbol{\theta}\cdot\widehat{\boldsymbol{k}})^2 - c^2\theta_0^2)\right) - \frac{i}{2}\left(\theta^0 \pm c\boldsymbol{\theta}\cdot\widehat{\boldsymbol{k}}\right)\,. \tag{9}$$

Notice the possibility of weak damping or anti–damping of plane waves and of both isotropic and anisotropic dispersion.

The group velocity corresponding to the dispersion relation (9) is

$$\boldsymbol{c}_{\rm g} = c\boldsymbol{\nabla}_{\boldsymbol{k}}{\rm Re}\,\omega = c\widehat{\boldsymbol{k}}\left(1 + \frac{1}{8|\boldsymbol{k}|^2}\left(c^2\theta_0^2 - 3(\boldsymbol{\theta}\cdot\widehat{\boldsymbol{k}})^2\right)\right) + c\frac{\boldsymbol{\theta}\cdot\widehat{\boldsymbol{k}}}{4|\boldsymbol{k}|^2}\boldsymbol{\theta} + \mathcal{O}(\theta^3/|\boldsymbol{k}|^3)\,. \tag{10}$$

Its modulus is

$$c_{\rm g} = c + \frac{c}{4|\boldsymbol{k}|^2}\left(c^2\theta_0^2 - (\boldsymbol{\theta}\cdot\widehat{\boldsymbol{k}})^2\right)\,. \tag{11}$$

The phase velocity implied by (9) is also anisotropic and depends on wavelength,

$$c_{\rm p} = \frac{{\rm Re}\,\omega}{|\boldsymbol{k}|} \approx c + \frac{c}{8|\boldsymbol{k}|^2}((\boldsymbol{\theta}\cdot\widehat{\boldsymbol{k}})^2 - c^2\theta_0^2)\,. \tag{12}$$

In the limit of small wavelengths both the group and phase velocities approach c so that this parameter has a clear operational meaning.

2.3 The field of a point charge

For a point charge q at rest $\boldsymbol{j} = 0$ and the modified Maxwell equations (4) and (5) take the form

$$\begin{aligned} 4\pi q\delta(\boldsymbol{x}) &= \boldsymbol{\nabla}\cdot\boldsymbol{E} + \boldsymbol{\theta}\cdot\boldsymbol{E} && (13)\\ 0 &= \boldsymbol{\nabla}\times\boldsymbol{B} + \frac{1}{c}\partial_t\boldsymbol{E} - \frac{1}{c}\theta_0\boldsymbol{E} + \boldsymbol{\theta}\times\boldsymbol{B}\,. && (14)\end{aligned}$$

Interestingly, when θ_0 is nonzero there is no static solution to these equations because of charge nonconservation. In that case, $\frac{d}{dt}q = \theta_0 q$ which implies a corresponding time dependence of the

electric field, $\frac{d}{dt}\boldsymbol{E} = \theta_0 \boldsymbol{E}$. Consequently, the terms in (14) involving the electric field cancel, so that $\boldsymbol{B} = 0$. We can then solve equation (13) by introducing a scalar potential, $\boldsymbol{E} = -\boldsymbol{\nabla}\phi$, to obtain

$$\Delta\phi + \boldsymbol{\theta}\cdot\boldsymbol{\nabla}\phi = 4\pi q\delta(\boldsymbol{x})\,. \tag{15}$$

The solution of this equation is [10]

$$\phi(\boldsymbol{x}) = -q\frac{e^{-\frac{1}{2}(\boldsymbol{\theta}\cdot\boldsymbol{x}+|\boldsymbol{\theta}|r)}}{r} = -q\frac{e^{-\frac{1}{2}|\boldsymbol{\theta}|r(1+\cos\vartheta)}}{r}\,, \tag{16}$$

where $r = |\boldsymbol{x}|$ and ϑ is the angle between $\boldsymbol{\theta}$ and the position vector $\boldsymbol{x}$. Note the anisotropic, Yukawa–like character of this potential when $|\boldsymbol{\theta}| \neq 0$.

The corresponding electric field is

$$\boldsymbol{E}(\boldsymbol{x}) = -q\boldsymbol{\nabla}\cdot\phi(\boldsymbol{x}) = -qe^{-\frac{1}{2}(\boldsymbol{\theta}\cdot\boldsymbol{x}+|\boldsymbol{\theta}|r)}\left(\frac{\boldsymbol{x}}{r^3} + \frac{1}{2}\left(\boldsymbol{\theta} + |\boldsymbol{\theta}|\frac{\boldsymbol{x}}{r}\right)\frac{1}{r}\right)\,. \tag{17}$$

3 The structure of ionic solids

In Michelson–Morley experiments light propagates back and forth along interferometer arms or back and forth within a resonant cavity. Since such structures are made of solids whose properties reflect the electromagnetic interaction between atoms we must consider the effect our modification of the Maxwell equations has on the structure of Michelson–Morley experimental apparatus. In this Letter we do so by considering the illustrative case of ionic crystalline solids. In this section we show that the our modified Maxwell equations can predict an orientation dependence of the separation between crystal planes and, thus, of the length of ionic solids.

As a simple model of an ionic crystal we take an infinite chain of alternating positive and negative ions with charges of magnitude q. To calculate this crystal's structure we proceed as in [15]. Our scalar potential (16) governs the electric interaction between ions. To stabilize the crystal there must also be a repulsive potential which we model by $\lambda e^{-r/\rho}$ where $\rho > 0$ and $\lambda > 0$ are parameters characterizing, respectively, the potential's range and strength. Fundamentally, this stabilizing potential is a reflection of the Pauli exclusion principle [15]. While one could consider the effect of conceivable modifications of quantum physics on the outcomes of Michelson–Morley experiments, here we consider only effects caused by our modifications of the Maxwell equations. Therefore, we take the parameters ρ and λ to be independent of θ_a.

The total energy for an ion in our infinite model crystal is

$$U = \sum_{n=1}^{\infty}\left(\lambda e^{-nr/\rho} + (-1)^n q^2\frac{e^{-\frac{1}{2}|\boldsymbol{\theta}|nr(1+\cos\vartheta)}}{nr}\right) + \sum_{n=1}^{\infty}\left(\lambda e^{-nr/\rho} + (-1)^n q^2\frac{e^{-\frac{1}{2}|\boldsymbol{\theta}|nr(1-\cos\vartheta)}}{nr}\right)\,, \tag{18}$$

where ϑ denotes the angle between our ionic chain and the vector field $\boldsymbol{\theta}$. The sum is easily computed,

$$U = \frac{2\lambda}{1-e^{-r/\rho}} - \frac{q^2}{r}\ln\left(1 + e^{-\frac{1}{2}|\boldsymbol{\theta}|r(1+\cos\vartheta)}\right) - \frac{q^2}{r}\ln\left(1 + e^{-\frac{1}{2}|\boldsymbol{\theta}|r(1-\cos\vartheta)}\right)\,. \tag{19}$$

The logarithms yield the Madelung constant which, in this case, depends on $\boldsymbol{\theta}$. The energy expression above reduces to the familiar result in the case $\boldsymbol{\theta} = 0$.

The equilibrium condition that determines the separation, R, between ions (crystal planes) is

$$0 = \left.\frac{dU(r)}{dr}\right|_R\,. \tag{20}$$

This is an implicit equation for R,

$$\begin{aligned} 0 \quad = \quad & -\frac{\lambda}{\rho}\frac{2e^{-R/\rho}}{\left(1-e^{-R/\rho}\right)^2} + \frac{q^2}{R^2}\ln\left(1+e^{-\frac{1}{2}|\boldsymbol{\theta}|R(1+\cos\vartheta)}\right) + \frac{1}{2}\frac{q^2}{R}\frac{|\boldsymbol{\theta}|(1+\cos\vartheta)e^{-\frac{1}{2}|\boldsymbol{\theta}|R(1+\cos\vartheta)}}{1+e^{-\frac{1}{2}|\boldsymbol{\theta}|R(1+\cos\vartheta)}} \\ & + \frac{q^2}{R^2}\ln\left(1+e^{-\frac{1}{2}|\boldsymbol{\theta}|R(1-\cos\vartheta)}\right) + \frac{1}{2}\frac{q^2}{R}\frac{|\boldsymbol{\theta}|(1-\cos\vartheta)e^{-\frac{1}{2}|\boldsymbol{\theta}|R(1-\cos\vartheta)}}{1+e^{-\frac{1}{2}|\boldsymbol{\theta}|R(1-\cos\vartheta)}}\,. \end{aligned} \tag{21}$$

which we can simplify because we are interested in the case of small $|\boldsymbol{\theta}|R$ and because R/ρ is large, implying $\frac{1}{\rho}\frac{e^{-R/\rho}}{\left(1-e^{-R/\rho}\right)^2} \approx \frac{1}{\rho}e^{-R/\rho}$. To leading order in $|\boldsymbol{\theta}|R$ the simplified equation is

$$R^2\left(e^{-R/\rho} + \frac{q^2}{32}\frac{\rho}{\lambda}|\boldsymbol{\theta}|^2(1+\cos^2\vartheta)\right) = q^2\frac{\rho}{\lambda}\ln 2\,. \tag{22}$$

To determine the fundamental scale R it is convenient to introduce R_0, the fundamental scale in the case $\boldsymbol{\theta} = 0$,

$$R_0^2 e^{-R_0/\rho} = q^2\frac{\rho}{\lambda}\ln 2\,. \tag{23}$$

Then, $R = R_0 + \delta R$ and solving for δR to leading order we obtain

$$\frac{\delta R}{R_0} = \frac{1}{32}\frac{\rho R_0|\boldsymbol{\theta}|^2}{\ln 2\,(1-2\rho/R_0)}(1+\cos^2\vartheta)\,, \tag{24}$$

where the charge q has been eliminated by using (23).

Clearly, when $|\boldsymbol{\theta}|$ is nonzero the fundamental crystal scale $R = R_0 + \delta R$ is orientation dependent. The overall length L of a solid with n crystal planes is

$$L(\vartheta) = nR_0\left(1+\frac{\delta R}{R_0}\right) = L_0\left(1+\frac{1}{32}\frac{\rho R_0|\boldsymbol{\theta}|^2}{\ln 2\,(1-2\rho/R_0)}(1+\cos^2\vartheta)\right)\,, \tag{25}$$

where $L = nR$ and $L_0 = nR_0$.

Note, in passing, that such orientation dependence of the length of solids implies that the spatial coordinates we have been using do not have the physical meaning one might have expected. This is of no real concern since we will computing physical observables that are, in effect, the result of a direct comparison of a body's extension to an electromagnetic wavelength. Note, too, that one might have chosen to consider the Bohr radius of a hydrogen atom as a fundamental standard of length. This has also been shown to depend on parameters of test theories encompassing modified Maxwell equations [16].

4 Predicting the outcome of a Michelson–Morley experiment

4.1 Interferometer experiments

The phase difference monitored in an interferometric Michelson–Morley experiment is $\phi = \omega\,\Delta t$, where Δt denotes the difference in time for propagation at the phase velocity along the interferometer's two arms. This is influenced by any anisotropy of the phase velocity of light as well as by any orientation dependence of the lengths of the interferometer's arms.

Our Eq.(12) gives the phase velocity as

$$c_{\mathrm{p}}(\vartheta) = c + \frac{c}{8|\boldsymbol{k}|^2}(|\boldsymbol{\theta}|^2\cos^2\vartheta - c^2\theta_0^2) \tag{26}$$

where ϑ is the angle between the interferometer arm the wave is propagating along and $\boldsymbol{\theta}$. Our Eq.(25) gives the length of each of the interferometer's arms as a function of its angle relative to $\boldsymbol{\theta}$. Consequently, the observed phase shift as a function of the angle ϑ of a chosen arm is

$$\begin{aligned}\Delta t &= \frac{L(\vartheta)}{c_{\mathrm{p}}(\vartheta)} - \frac{L(\vartheta+\frac{\pi}{2})}{c_{\mathrm{p}}(\vartheta+\frac{\pi}{2})}\\ &= \frac{L_0|\boldsymbol{\theta}|^2}{8c}\left(\frac{1}{4}\frac{\rho R_0}{\ln 2\,(1-2\rho/R_0)} - \frac{c^2}{\omega^2}\right)(\cos^2\vartheta - \sin^2\vartheta) + \mathcal{O}(|\boldsymbol{\theta}|^4)\,. \end{aligned}\tag{27}$$

Notice that even when $|\boldsymbol{\theta}| \neq 0$ it is conceivable that there will be *no* interference signal. It is possible for the effects of the anisotropic phase velocity and the orientation dependence of the length of the interferometer's arms to cancel at a particular frequency, namely, the one that satisfies

$$\frac{1}{\omega^2} - \frac{1}{4c^2} \frac{\rho R_0}{\ln 2\,(1 - 2\rho/R_0)} = 0\,. \tag{28}$$

Typical crystals have $\rho \sim 0.1\ R_0$ and $R_0 \sim 10^{-10}$ m implying a cancellation frequency of

$$\omega = 2c\sqrt{\frac{0.8 \ln 2}{0.1\ R_0^2}} = 1.4 \times 10^{19}\ \text{Hz}\,. \tag{29}$$

Since interferometric Michelson–Morley experiments are performed with visible light having frequencies much lower than this the cancellation of competing effects is not a problem in practice.

4.2 Resonant cavity experiments

The frequency monitored in a resonant–cavity Michelson–Morley experiment is influenced by any anisotropy of the phase velocity of light as well as by any orientation dependence of the cavity's length. The phase velocity governs the relationship between the resonant radiation's frequency and wavelength while the cavity's length determines the resonant wavelength.

For a standing wave in a cavity we have

$$|\boldsymbol{k}(\vartheta)| = \frac{\pi n}{L(\vartheta)}\,, \tag{30}$$

where $n = 1, 2, 3, \ldots$ is the number of half wavelengths in the standing wave. The corresponding resonant angular frequencies are

$$\begin{aligned}
\omega(\vartheta) &= |\boldsymbol{k}(\vartheta)|c\left(1 + \frac{1}{8|\boldsymbol{k}|^2}(|\boldsymbol{\theta}|^2 \cos^2\vartheta - \theta_0^2)\right) \\
&= \frac{\pi n c}{L_0}\left(1 - \frac{L_0^2}{32\pi^2 n^2}\theta_0^2 - \frac{1}{32}\frac{\rho R_0 |\boldsymbol{\theta}|^2}{\ln 2\,(1 - 2\rho/R_0)}\right. \\
&\qquad \left. + \frac{|\boldsymbol{\theta}|^2}{32}\left(\frac{L_0^2}{\pi^2 n^2} - \frac{\rho R_0}{\ln 2\,(1 - 2\rho/R_0)}\right)\cos^2\vartheta\right) + \mathcal{O}(|\boldsymbol{\theta}|^4)\,.
\end{aligned} \tag{31}$$

The amplitude of the fractional variation in resonant frequency as the cavity rotates relative to $\boldsymbol{\theta}$ is, therefore,

$$\frac{\delta\omega}{\omega} = \frac{|\boldsymbol{\theta}|^2}{16}\left(\frac{L_0^2}{\pi^2 n^2} - \frac{\rho R_0}{\ln 2\,(1 - 2\rho/R_0)}\right)\,. \tag{32}$$

Once again, even when $|\boldsymbol{\theta}| \neq 0$ it is conceivable that the effects of an anisotropic speed of light and of an orientation dependence of the length of solid bodies can cancel. In this case the condition for cancellation is

$$\frac{L_0^2}{\pi^2 n^2} = \frac{\rho R_0}{\ln 2\,(1 - 2\rho/R_0)} \approx 1.8 \times 10^{-21}\ m^2\,. \tag{33}$$

For a mean cavity length of, say, $L_0 \sim 30$ cm this implies $n \approx 2.3 \times 10^9$. The corresponding mean resonant frequency is $\nu_0 = cn/(2L_0) \sim 1.1 \times 10^{18}$ Hz. Since resonant cavity Michelson–Morley experiments are performed with microwaves having frequencies much lower than this the cancellation of competing effects is not a problem in practice.

5 Conclusions and outlook

The design and the interpretation of the results of experimental tests of Special Relativity demand consideration of consistent, physically reasonable alternatives to familiar relativistic dynamics. One can only design experiments to search for differences between the predictions of special relativistic and alternative dynamics when one has determined the predictions of both.

In this Letter we have shown that the alternative model of electrodynamics based on the modified Maxwell equations (3) can predict both an anisotropic speed of light and an orientation dependence of the length of solid bodies. This combination of predictions complicates the interpretation of interferometric and resonant–cavity Michelson–Morley experiments because, in principle, the effect of orientation dependence of the lengths of interferometer arms and cavity resonators can cancel the effect of an anisotropic speed of light. Both effects must be accounted for to obtain a reliable interpretation of the results of a Michelson–Morley experiment.

We have used the simplest possible model of ionic crystals to estimate the orientation dependence of the lengths of solid bodies predicted by the modified electrodynamics (3). While estimates based on more sophisticated models of other types of solids need to be made, our estimates suggest that for this modified dynamics the effect of an anisotropic speed of light dominates that of orientation dependence of the length of solid bodies in past and proposed Michelson–Morley experiments. For example, the precise microwave experiment of Brillet and Hall [4] employed a glass–ceramic cavity 0.305 m long operated at a resonant frequency of roughly 10^{14} Hz. Taking the estimates of the previous section as an indication of the order of magnitude of any predicted orientation dependence of the length of the glass–ceramic cavity, even though it is not an ionic solid body, we see that the operating frequency is four orders of magnitude below that for which the effect of orientation dependent cavity length would be large enough to compensate for the effect of the predicted anisotropic speed of light. Similar considerations establish that the effect of orientation dependent cavity length is negligible in the proposed SUMO [5] and OPTIS [6] experiments. We note that the prediction (32) and the target precision of these proposed experiments suggests that they will be able to impose the constraint $|\boldsymbol{\theta}| \lesssim 0.3\ \mathrm{m}^{-1}$. Note that is not competitive with astrophysical constaints [10].

We will discuss other predictions of the alternative electrodynamics (3) elsewhere [10]. Similar analyses can be performed for the more general model (2) which can predict birefringence and can be expected to predict more complicated orientation dependence of the speed of light and the lengths of solid bodies.

One final remark, the results of Hughes–Drever experiments like [17] provide some justification for our assumption in section 3 that quantum physics remains intrinsically isotropic in the alternative models of dynamics we have considered. Such experiments can, for example, be shown to tightly constrain any anisotropy of the inertial masses of particles that appear in the Schrödinger equation [18].

Acknowledgement

C.L. thanks Ken Nordtvedt, Gerhard Schäfer, and Stephan Schiller for very useful discussions and the Optikzentrum of the University of Konstanz, where part of this work was written, for financial support.

References

[1] A.A. Michelson and E.W. Morley. On the relative motion of the Earth and the luminiferous ether. *Am. J. Sci.*, 34:333, 1887.

[2] A. Einstein. Zur Elektrodynamik bewegter Körper. *Ann. Physik*, 17:891, 1905.

[3] H.P. Robertson. Postulate versus observation in the Special Theory of Relativity. *Rev. Mod. Phys.*, 21:378, 1949.

[4] A. Brillet and J.L. Hall. Improved laser test of the isotropy of space. *Phys. Rev. Lett.*, 42:549, 1979.

[5] S. Buchman, J.P. Turneaure, J.A. Lipa, M. Dong, K.M. Cumbernack, and Wang. S. A superconducting microwave oscillator clock for use on the space station. *Proceedings of the IEEE International Frequency Symposium*, IEEE:534, 1998.

[6] C. Lämmerzahl, S. Schiller, H.-J. Dittus, and A. Peters. OPTIS – satellite based optical tests of special and general relativity. University of Düsseldorf.

[7] C. Lämmerzahl, R. Puntigan, and F.W. Hehl. Can the electromagnetic field couple to post–Riemannian structures? In T. Piran and R. Ruffuni, editors, *Proceedings of the Eight Marcel Grossmann Meeting on General Relativity*, page 457. World Scientific, Singapore, 1999.

[8] M.P. Haugan and C. Lämmerzahl. On the experimental foundations of the Maxwell equations. *Ann. Phys. (Leipzig)*, 9:119, 2000.

[9] M.P. Haugan and Lämmerzahl. Principles of equivalence: Their role in gravitation physics and experiments that test them. In C. Lämmerzahl, C.W.F. Everitt, and F.W. Hehl, editors, *Gyros, Clocks, and Interferometers: Testing Relativistic Gravity in Space*, page to appear. Springer–Verlag, Berlin, 2000.

[10] M. Haugan and C. Lämmerzahl. On the mass of the photon. in preparation.

[11] C. Itzykson and J.-B. Zuber. *Quantum Field Theory.* McGraw–Hill, New York, 1980.

[12] S.L. Dubovsky, V.A. Rubakov, and P.G. Tinyakov. Is the electric charge conserved in brane world? gr–qc/0007179.

[13] E.R. Williams, J.E. Faller, and H.A. Hill. New experimental test of Coulomb's law: A laboratory upper limit on the photon rest mass. *Phys. Rev. Lett.*, 26:721, 1971.

[14] B.E. Schaefer. Severe limits on variations of the speed of light with frequency. *Phys. Rev. Lett.*, 82:4964, 1999.

[15] Ch. Kittel. *Introduction to solid state physics.* Wiley, New York, 1971.

[16] C.M. Will. Gravitational red–shift measurements as tests of nonmetric theories of gravity. *Phys. Rev.*, D 10:2330, 1974.

[17] T.E. Chupp, R.J. Hoara, R.A. Loveman, E.R. Oteiza, J.M. Richardson, and M.E. Wagshul. Results of a new test of local Lorentz invariance: A search for mass anisotropy in ^{21}Ne. *Phys. Rev. Lett.*, 63:1541, 1989.

[18] C. Lämmerzahl. Quantum tests of foundations of general relativity. *Class. Quantum Grav.*, 14:13, 1998.